Supplemental information

Sector coupling leading to low-carbon production of power and chemicals in China

Yinan Li [1], Lanyu Li [2, 3], Chuan Zhang [4], Yingru Zhao [5], Xiaonan Wang [2, *]

[1] Department of Chemical and Biomolecular Engineering, National University of Singapore, Singapore 117585, Singapore

[2] Department of Chemical Engineering, Tsinghua University, Beijing 100084, China

[3] School of Economics and Management, Tsinghua University, Beijing 100084, China

[4] Institute of Energy, Peking University, Beijing 100871, China

[5] College of Energy, Xiamen University, Xiamen, China

[*] Corresponding author: wangxiaonan@tsinghua.edu.cn

1. Optimization model formulation

The detailed data sources and procedures for technology modeling and VRE potential estimation are provided in later sections of Supplemental Information while the formulation of optimization model is described below. In the upper-level capacity expansion model, net present cost over the entire planning horizon of 20 years is minimized as shown in Equations (1) – (8).

$$\min_{x,y,z} \sum_{t} \frac{1}{(1+R)^{t-t_0}} \left(CX_t + CXT_t + FX_t + FXT_t + VXE_t + VXC_t + VXT_t\right) \#(1)$$

$$CX_t = \sum_{i,j,\tau \le t \ \wedge \ \tau + CT_{i,j} > t} \left(\frac{CAPEX_{\tau,i,j}}{CT_{i,j}}\right)\left(x_{\tau,i,j} + EXCAP_{\tau,i,j}\right) \quad \forall t \#(2)$$

$$CXT_t = \sum_{i,i',\tau \le t \ \wedge \ \tau + CT_{i,i'} > t} \left(\frac{CAPEX_{\tau,i,i'}}{CT_{i,i'}}\right)\left(x_{\tau,i,i'} + EXCAP_{\tau,i,i'}\right) \quad \forall t \#(3)$$

$$FX_t = \sum_{i,j,\tau + CT_{i,j} \le t \ \wedge \ \tau + CT_{i,j} + LT_{i,j} > t} \left(FOPEX_{\tau,i,j}\right)\left(x_{\tau,i,j} + EXCAP_{\tau,i,j}\right) \quad \forall t \#(4)$$

$$FXT_t = \sum_{i,i',\tau + CT_{i,i'} \le t \ \wedge \ \tau + CT_{i,i'} + LT_{i,i'} > t} \left(FOPEX_{\tau,i,i'}\right)\left(x_{\tau,i,i'} + EXCAP_{\tau,i,i'}\right) \quad \forall t \#(5)$$

$$VXE_t = \sum_{d,h,i,j \in J_E} \left(\Delta D_d\right)\left(\Delta H_h\right)\left(VOPEX_{t,i,j}\right) y_{t,d,h,i,j} + \sum_{d,h,i,j \in J_{ED}} \left(\Delta D_d\right)\left(SSEX_{t,i,j}\right)\left(UT_{i,j}\right)\left(y^{ON}_{t,d,h,i,j} + y^{OFF}_{t,d,h,i,j}\right) \quad \forall t \#(6)$$

$$VXC_t = \sum_{d,i,j \in J_C} \left(\Delta D_d\right)\left(VOPEX_{t,i,j}\right) y_{t,d,i,j} \quad \forall t \#(7)$$

$$VXT_t = \sum_{i,i'} \left(FREIGHT_t\right)\left(DIST_{i,i'}\right)\left(z^{M}_{t,i,i'} + z^{A}_{t,i,i'}\right) \quad \forall t \#(8)$$

where CX_t and CXT_t are the capital costs of production and transmission technologies in year t, respectively. t_0 denotes the starting year of a planning horizon and R is the discount rate taken to be 8% in this work. Similarly, FX_t and FXT_t represent fixed costs and VXT_t is the freight cost due to transport of chemicals. Variable operating costs are split into two parts for electricity (VXE_t) and chemical (VXC_t) related technologies given their difference in operational flexibility. For decision variables, $x_{t,i,j}$ and $x_{t,i,i'}$ are the construction of new production facilities for technology j in province i and transmission lines between provinces i and i' in year t, respectively. $y_{t,d,h,i,j}$ denotes the operation of technology j in province i for representative day d and hour h (omitted in $y_{t,d,i,j}$) in year t and the number of flexibly operable units to turn on and off are represented by $y^{ON}_{t,d,h,i,j}$ and $y^{OFF}_{t,d,h,i,j}$, respectively. For pumped hydro storage, all operating cost is assumed to happen in the discharging phase covered by $y_{t,d,h,i,j}$ while the charging operation is represented by $y^{PHC}_{t,d,h,i,j}$. Here, $z^{E}_{t,d,h,i,i'}$ is the power transmission from province i to i' for representative day d and hour h in year t, while $z^{M}_{t,i,i'}$ and $z^{A}_{t,i,i'}$ are the transport of methanol and ammonia from province i to i' in year t, respectively. Regarding model parameters, $CAPEX_{t,i,j}$, $FOPEX_{t,i,j}$ and $VOPEX_{t,i,j}$ are capital, fixed and variable costs of technology j in province i for year t, respectively. $EXCAP_{t,i,j}$ denotes the existing capacity of technology j in province i constructed in year t, which is always updated by solution of $x_{t,i,j}$ across iterations of receding horizon optimization. $CT_{i,j}$ and $LT_{i,j}$ represent the plant construction time and lifetime of technology j in province i, respectively. In this work, it is assumed that construction costs and emissions are distributed uniformly over the construction period while fixed costs occur every year during the plant lifetime. $CAPEX_{\tau,i,i'}$, $FOPEX_{\tau,i,i'}$, $EXCAP_{t,i,i'}$, $CT_{i,i'}$ and $LT_{i,i'}$ are similarly defined for transmission lines between provinces i and i'. Set J_E represents electricity-related technologies including all power sector technologies and electrolysis, among which dispatchable ones, namely thermal generators and water electrolyzer, are further involved in J_{ED}. ΔD_d and ΔH_h are the length of representative day d (in days) and hour h (in hours), serving as scaling factors to estimate annual cost based on selected representative samples. $SSEX_{t,i,j}$ is the start-up/shut-down cost of technology j in province i for year t while $UT_{i,j}$ represents the unit size of dispatchable technologies. Set J_C includes those less flexible technologies, i.e., fossil and hydrogen-based chemicals production as well as DAC. Since representative days are selected on the basis of one per season (upper-level model) or one per month (lower-level model), the operation status of those technologies in J_C is only varied across seasons/months in this work. For transport cost, $FREIGHT_t$ is the freight rate in year t and $DIST_{i,i'}$ denotes the inter-provincial distance between provinces i and i'. In the lower-level model, given that only annual operation cost is minimized, the CX_t, CXT_t, FX_t and FXT_t terms are excluded from Equation (1) and the (undiscounted) remaining terms are only optimized over decision variables y and z.

Final product demands must be satisfied by the nexus at different temporal resolutions. For electricity, provincial grid demand profile is specified for each representative hour and day every year. Considering the relatively high safety and low cost of long-term storage of methanol and ammonia, chemical supply is only required to meet annually aggregated demand. Also, the consumption of hydrogen and captured carbon dioxide (CO_2) is balanced within the system boundary as reflected in Equations (9) – (13).

$$\sum_{j \in J_E} (ELEC_{i,j}) y_{t,d,h,i,j} - y^{PHC}_{t,d,h,i,j} + \frac{1}{24} \sum_{j \in J_C} (ELEC_{i,j}) y_{t,d,i,j} - \sum_{i'} z^{E}_{t,d,h,i,i'} + \sum_{i'} \left(1 - (LOSS)\left(DIST_{i,i'}\right)\right) z^{E}_{t,d,h,i',i} \geq (1 + ELMG)\left(ELDM_{t,d,h,i}\right) \quad \forall t,d,h,i \# (9)$$

$$\sum_{d,j \in J_C} (\Delta D_d)\left(METH_{i,j}\right) y_{t,d,i,j} - \sum_{i'} z^{M}_{t,i,i'} + \sum_{i'} z^{M}_{t,i',i} \geq (1 + MEMG)\left(MEDM_{t,i}\right) \quad \forall t,i \# (10)$$

$$\sum_{d,j \in J_C} (\Delta D_d)\left(AMMO_{i,j}\right) y_{t,d,i,j} - \sum_{i'} z^{A}_{t,i,i'} + \sum_{i'} z^{A}_{t,i',i} \geq (1 + AMMG)\left(AMDM_{t,i}\right) \quad \forall t,i \# (11)$$

$$\sum_{h,j \in J_E} (\Delta H_h)\left(HYDR_{i,j}\right) y_{t,d,h,i,j} + \sum_{j \in J_C} \left(HYDR_{i,j}\right) y_{t,i,j} \geq 0 \quad \forall t,d,i \# (12)$$

$$\sum_{h,j \in J_E} (\Delta H_h)\left(CARB_{i,j}\right) y_{t,d,h,i,j} + \sum_{j \in J_C} \left(CARB_{i,j}\right) y_{t,i,j} \geq 0 \quad \forall t,d,i \# (13)$$

where $ELEC_{i,j}$, $METH_{i,j}$, $AMMO_{i,j}$, $HYDR_{i,j}$ and $CARB_{i,j}$ are mass balance coefficients denoting respectively the amount of electricity, methanol, ammonia, hydrogen and captured CO_2 supplied per unit operation of technology j in province i with negative values for consumption. $ELDM_{t,d,h,i}$, $MEDM_{t,i}$ and $AMDM_{t,i}$ represent electricity, methanol and ammonia demands of province i in year t with power demand profiles further specified for representative day d and hour h. $ELMG$, $MEMG$ and $AMMG$ denote safety margins for electricity, methanol and ammonia demands set to be 10%, 2% and 2%, respectively, in the upper-level model and zero in the lower-level model. Besides demand satisfaction, a series of technology operation constraints is also enforced in the model. Utilizable capacity can firstly be calculated from Equations (14) – (15).

$$CAP_{t,i,j} = \sum_{\tau + CT_{i,j} \leq t \ \wedge \ \tau + CT_{i,j} + LT_{i,j} > t} x_{\tau,i,j} + EXCAP_{\tau,i,j} \quad \forall t,i,j \# (14)$$

$$CAP_{t,i,i'} = \sum_{i,i',\tau + CT_{i,i'} \leq t \ \wedge \ \tau + CT_{i,i'} + LT_{i,i'} > t} x_{\tau,i,i'} + EXCAP_{\tau,i,i'} \quad \forall t,i,i' \# (15)$$

where $CAP_{t,i,j}$ and $CAP_{t,i,i'}$ represent the capacity of technology j in province i and transmission

line between provinces i and i', respectively, in year t. Given that the values of $x_{t,i,j}$ and $x_{t,i,i'}$ are copied into $EXCAP_{t,i,j}$ and $EXCAP_{t,i,i'}$ across iterations during the receding horizon optimization of capacity expansion model, only the $EXCAP$ parameters are needed in capacity calculation for the lower-level model. The unit commitment of dispatchable technologies in J_{ED} is modeled by Equations (16) – (22) below with all integer variables relaxed to be continuous for computational tractability. For large-scale models, such relaxation has been shown to be acceptable in terms of solution accuracy [1,2].

$$ON_{t,d,h,i,j} \leq \frac{CAP_{t,i,j}}{UT_{i,j}} \quad \forall t,d,h,i,j \in J_{ED} \#(16)$$

$$ON_{t,d,h,i,j} - ON_{t,d,h-1,i,j} = y^{ON}_{t,d,h,i,j} - y^{OFF}_{t,d,h,i,j} \quad \forall t,d,h,i,j \in J_{ED} \#(17)$$

$$\sum_{h-UP_{i,j} < \eta \leq h} y^{ON}_{t,d,\eta,i,j} \leq ON_{t,d,h,i,j} \quad \forall t,d,h,i,j \in J_{ED} \quad \#(18)$$

$$\sum_{h-DN_{i,j} < \eta \leq h} y^{OFF}_{t,d,\eta,i,j} \leq \frac{CAP_{t,i,j}}{UT_{i,j}} - ON_{t,d,h,i,j} \quad \forall t,d,h,i,j \in J_{ED} \quad \#(19)$$

$$(SL_{i,j})(UT_{i,j})ON_{t,d,h,i,j} \leq y_{t,d,h,i,j} \leq (UT_{i,j})ON_{t,d,h,i,j} \quad \forall t,d,h,i,j \in J_{ED} \#(20)$$

$$y_{t,d,h,i,j} - y_{t,d,h-1,i,j} \leq (RU_{i,j})(UT_{i,j})\left(ON_{t,d,h,i,j} - y^{ON}_{t,d,h,i,j}\right) + \max\left(SL_{i,j}, RU_{i,j}\right)(UT_{i,j})y^{ON}_{t,d,h,i,j} - (SL_{i,j})(UT_{i,j})y^{OFF}_{t,d,h,i,j} \quad \forall t,d,h,i,j \in J_{ED} \#(21)$$

$$y_{t,d,h-1,i,j} - y_{t,d,h,i,j} \leq (RD_{i,j})(UT_{i,j})\left(ON_{t,d,h,i,j} - y^{ON}_{t,d,h,i,j}\right) + \max\left(SL_{i,j}, RD_{i,j}\right)(UT_{i,j})y^{OFF}_{t,d,h,i,j} - (SL_{i,j})(UT_{i,j})y^{ON}_{t,d,h,i,j} \quad \forall t,d,h,i,j \in J_{ED} \#(22)$$

where $ON_{t,d,h,i,j}$ is the number of turned-on (i.e., in operation) units of technology j in province i during representative day d and hour h in year t. $UP_{i,j}$ and $DN_{i,j}$ are the up and down time of technology j in province i, respectively. In the upper-level model, a time interval between representative hours (i.e., ΔH_h) of 3 hours is used, so $UP_{i,j}$ and $DN_{i,j}$ are set to one for approximation. In the lower-level model, however, a time interval of one hour is used and the up and down time assume their actual values in hours. $SL_{i,j}$ is the minimum stable operation level of technology j in province i while $RU_{i,j}$ and $RD_{i,j}$ represent the maximum ramping up and down rate of technology j in province i, respectively. Note that the $h-1$ above denotes the previous hour index of $h \in H$ in a round-robin manner. In this work, nuclear and hydro electricity generation are assumed to provide baseload [3] with seasonal/monthly variation in hydropower reflected by corresponding capacity factors as shown in Equations (23) – (24). For other VREs, the resource availability is location specific, so capacity factors can differ between existing and future installations as in Equation (25).

$$y_{t,d,h,i,j} = CAP_{t,i,j} \quad \forall t,d,h,i,j = \text{nuclear power} \#(23)$$

$$y_{t,d,h,i,j} = (CF_{d,i,j})CAP_{t,i,j} \quad \forall t,d,h,i,j = \text{hydro power} \#(24)$$

$$y_{t,d,h,i,j} = (ECF_{t,d,h,i,j})(RC_{t,i,j}) + (FCF_{t,d,h,i,j})(CAP_{t,i,j} - RC_{t,i,j}) \quad \forall t,d,h,i,j \in \{\text{onshore wind, offshore wind, solar power}\} \#(25)$$

where $CF_{d,i,j}$ is the capacity factor of technology j in province i for representative day d. $ECF_{t,d,h,i,j}$ and $FCF_{t,d,h,i,j}$ are the location averaged capacity factors of existing and future installations of technology j in province i for representative day d and hour h in year t, respectively. Detailed site selection criteria for new VRE installation are beyond the scope of this work and instead, a simple heuristic is assumed that locations with higher annual generation are developed earlier in a province. $RC_{t,i,j}$ denotes the existing renewable capacity before a planning horizon calculated with Equation (14) without the $x_{t,i,j}$ term. For pumped hydro storage, the following constraints are considered in Equations (26) – (29).

$$SOC_{t,d,h,i,j} = SOC_{t,d,h-1,i,j} + (\Delta H_h)(EFF_{i,j})y^{PHC}_{t,d,h,i,j} - (\Delta H_h)\left(\frac{1}{EFF_{i,j}}\right)y_{t,d,h,i,j}$$
$$\forall t,d,h,i,j = \text{pumped hydro} \quad (26)$$

$$y^{PHC}_{t,d,h,i,j} \leq CAP_{t,i,j} \quad \forall t,d,h,i,j = \text{pumped hydro} \quad (27)$$

$$y_{t,d,h,i,j} \leq CAP_{t,i,j} \quad \forall t,d,h,i,j = \text{pumped hydro} \quad (28)$$

$$SOC_{t,d,h,i,j} \geq 20\% * 6 * CAP_{t,i,j} \quad \forall t,d,h,i,j = \text{pumped hydro} \quad (29)$$

where $SOC_{t,d,h,i,j}$ is the state-of-charge (SOC) of storage technology j in province i for representative day d and hour h in year t while $EFF_{i,j}$ denotes the efficiency of technology j in province i. Equation (29) sets the minimum SOC of pumped hydro facilities for 6-hour continuous discharging at 20% capacity [4]. Lastly, the operation of technologies in J_C and power transmission across provinces are modeled with Equations (30) – (31). For simplicity, bidirectional transmission is assumed in this work.

$$y_{t,d,i,j} \leq CAP_{t,i,j} \quad \forall t,d,i,j \in J_C \quad (30)$$

$$z^{E}_{t,d,h,i,i'} \leq CAP_{t,i,i'} + CAP_{t,i',i} \quad \forall t,d,h,i,j \quad (31)$$

The potential and growth rate of technologies are constrained by Equations (32) – (34) below.

$$CAP_{t,i,j} \leq POT_{t,i,j} \quad \forall t,i,j \quad (32)$$

$$\sum_i x_{t,i,j} \leq AGR_j \quad \forall t,j \quad (33)$$

$$\sum_i x_{t,i,j} \leq (RGR_j)\sum_i CAP_{t,i,j} \quad \forall t,j \quad (34)$$

where $POT_{t,i,j}$ denotes the potential of technology j in province t by year t. AGR_j and RGR_j represent the absolute and relative growth rate of technology j, respectively. In this work, positive and negative greenhouse gas (GHG) emissions of the proposed electricity-chemical nexus are tracked by Equations (35) – (40) and constrained by emission reduction pathway towards carbon neutrality as in Equation (41).

$$PE_t = CE_t + CET_t + OE_t + OET_t \quad \forall t \quad (35)$$

$$CE_t = \sum_{i,j,\tau \leq t \ \wedge\ \tau + CT_{i,j} > t} \left(\frac{CAPEM_{i,j}}{CT_{i,j}}\right)(x_{\tau,i,j} + EXCAP_{\tau,i,j}) \quad \forall t \quad (36)$$

$$CET_t = \sum_{i,i',\tau \le t \wedge \tau + CT_{i,i'} > t} \left(\frac{CAPEM_{i,i'}}{CT_{i,i'}} \right) \left(x_{\tau,i,i'} + EXCAP_{\tau,i,i'} \right) \quad \forall t \#(37)$$

$$OE_t = \sum_{d,h,i,j \in J_E} (\Delta D_d)(\Delta H_h)(POPEM_{i,j}) y_{t,d,h,i,j} + \sum_{d,i,j \in J_C} (\Delta D_d)(POPEM_{i,j}) y_{t,d,i,j} \quad \forall t \#(38)$$

$$OET_t = \sum_{i,i'} \left(TREM_{i,i'} \right) \left(z^{M}_{t,i,i'} + z^{A}_{t,i,i'} \right) \quad \forall t \#(39)$$

$$NE_t = \sum_{d,h,i,j \in J_E} (\Delta D_d)(\Delta H_h)(NOPEM_{i,j}) y_{t,d,h,i,j} + \sum_{d,i,j \in J_C} (\Delta D_d)(NOPEM_{i,j}) y_{t,d,i,j} \quad \forall t \#(40)$$

$$PE_t + NE_t \le TGT_t \quad \forall t \#(41)$$

where PE_t and NE_t denote total positive and negative GHG emissions in year t, respectively, while TGT_t represents the emission target for year t. Positive emissions can be further broken down into construction and operation phases due to production and transfer activities as listed by Equations (36) – (39) above. $CAPEM_{i,j}$ and $CAPEM_{i,i'}$ are unit facility construction GHG emissions of technology j in province i and transmission line between provinces i and i', respectively. The positive and negative emissions during operation phase of technology j in province i are denoted by $POPEM_{i,j}$ and $NOPEM_{i,j}$, respectively, while $TREM_{i,i'}$ represents the (positive) road transport emissions from province i to i'. Similar to capacity calculation, since $x_{t,i,j}$ and $x_{t,i,i'}$ are saved in $EXCAP_{t,i,j}$ and $EXCAP_{t,i,i'}$ after solving the upper-level model, only the latter parameters are needed for the lower-level model. In fact, CE_t and CET_t are sunk emissions and can thus be subtracted from TGT_t in the annual operation model.

Finally, given the spatially and temporally varying nature of electricity generation mix in different provinces during different hours of a year, the carbon intensity of electricity can be estimated with a pooled network flow model as shown in Equations (42) – (43) after solving the aforementioned bi-level optimization framework.

$$\left(CI^{S}_{t,d,h,i} \right)\left(SOC_{t,d,h,i,j} \right) = \left(CI^{S}_{t,d,h-1,i} \right)\left(SOC_{t,d,h-1,i,j} \right) + \left(CI^{E}_{t,d,h,i} \right)(\Delta H_h)\left(EFF_{i,j} \right)\left(y^{PHC}_{t,d,h,i,j} \right) - \left(CI^{S}_{t,d,h-1,i} \right)(\Delta H_h)\left(\frac{y_{t,d,h,i,j}}{EFF_{i,j}} \right) \quad \forall t,d,h,i,j = \text{pumped hydro} \#(42)$$

$$\left(CI^{E}_{t,d,h,i} \right)\left(\sum_{j \in J_{EG} \cup J_{ES}} y_{t,d,h,i,j} + \sum_{i'} \left(1 - (LOSS)\left(DIST_{i',i} \right) \right) z^{E}_{t,d,h,i',i} \right) = \sum_{j \in J_{EG}} (IM_{i,j}) y_{t,d,h,i,j} + \sum_{j \in J_{ES}} \left(CI^{S}_{t,d,h-1,i} \right) y_{t,d,h,i,j} + \sum_{i'} \left(CI^{E}_{t,d,h,i'} \right)\left(1 - (LOSS)\left(DIST_{i',i} \right) \right) z^{E}_{t,d,h,i',i} \quad \forall t,d,h,i \#(43)$$

where $CI^{S}_{t,d,h,i}$ and $CI^{E}_{t,d,h,i}$ denote the average carbon intensities of stored and generated electricity in province i for representative day d and hour h in year t, respectively. $IM_{i,j}$ is the life cycle carbon intensity of technology j in province i. Set J_{EG} involves all power generation technologies and J_{ES} only includes pumped hydro storage.

2. Data sources

The data sources of model parameters are listed in Table 1 below excluding those on technology emission and wind and solar modeling that require additional processing and will be detailed in subsequent contents. For mature technologies, future capital and fixed costs are assumed to maintain at the current levels while for emerging technologies, those values are updated across iterations with the corresponding (one-factor) technology learning rates as shown in Equations (44) – (45). The future variable operating costs of fuel-dependent technologies are determined based on future fuel price predictions while for fuel-independent counterparts, the current values are assumed for the future as well.

$$CAPEX_{t,i,j} = CAPEX_{t_0,i,j}\left(\frac{CUMCAP_{t,j}}{CUMCAP_{t_0,j}}\right)^{b_j} \#(44)$$

$$LR_j = 1 - 2^{b_j} \#(45)$$

where $CUMCAP_{t,j}$ and $CUMCAP_{t_0,j}$ denote the national cumulative capacity installation of technology j by year t and some reference year t_0, respectively. b_j is the learning elasticity of technology j which is usually a negative value and LR_j is the corresponding learning rate.

Table 1: Data sources of model parameters

Parameter	Specific Index (if any)	Source
$CAPEX_{t,i,j}$	j=coal, natural gas, nuclear electricity	5
	t=current; j=coal-CCS, natural gas-CCS, hydro, onshore wind, offshore wind, solar, biomass, biomass-CCS electricity	5
	t=current; j=pumped hydro storage	6
	j=coal, coke-oven gas, natural gas methanol	7,8
	t=current; j=hydrogen methanol	8
	j=coal, coke-oven gas, natural gas ammonia	9,10
	t=current; j=hydrogen ammonia	11
	t=current, future; j=water electrolysis	12
	t=current; j=direct air capture	13
$CAPEX'_{t,i,i}$		14
$FOPEX_{t,i,j}$	j=coal, natural gas, nuclear electricity	5
	t=current; j=coal-CCS, natural gas-CCS, hydro, onshore wind, offshore	5

	wind, solar, biomass, biomass-CCS electricity	
	t=current; j=pumped hydro storage	6
	j=coal, coke-oven gas, natural gas methanol	15
	t=current; j=hydrogen methanol	8
	j=coal, coke-oven gas, natural gas ammonia	16
	t=current; j=hydrogen ammonia	11
	t=current, future; j=water electrolysis	12
	t=current; j=direct air capture	13
$FOPEX_{t,i,i'}$		17
LR_j	j=coal-CCS, natural gas-CCS, biomass-CCS electricity, pumped hydro storage	18
	j=hydro, onshore wind, offshore wind, solar, biomass electricity	5
	j=hydrogen methanol, hydrogen ammonia, direct air capture	19
$VOPEX_{t,i,j}$	t=current; j=coal, coal-CCS, natural gas, natural gas-CCS electricity	5
	t=current, future; j=nuclear electricity	20
	j=hydro, onshore wind, offshore wind, solar electricity, pumped hydro storage	5
	t=current; j=biomass, biomass-CCS electricity	21
	t=future; j=biomass, biomass-CCS electricity	22
	t=current; j=coal, coke-oven gas, natural gas, hydrogen methanol	15
	t=current; j=coal, coke-oven gas, natural gas, hydrogen ammonia	16
	t=current, future; j=water electrolysis	12
	t=current; j=direct air capture	13
	t=future; j= coal, coal-CCS, natural gas, natural gas-CCS electricity, coal, coke-oven gas, natural gas, hydrogen methanol, coal, coke-oven gas, natural gas, hydrogen ammonia, direct air capture	23
$FREIGHT_t$	t=current	15
	t=future	24
$DIST_{i,i'}$		15
$CT_{i,j}$	j=coal, coal-CCS, natural gas, natural gas-CCS, nuclear electricity	20
	j=hydro, onshore wind, offshore wind, solar, biomass, biomass-CCS electricity, pumped hydro storage	5
	j=coal, coke-oven gas, natural gas, hydrogen methanol	7,8
	j=coal, coke-oven gas, natural gas, hydrogen ammonia	9,10
	j=water electrolysis	12
	j=direct air capture	13
$CT_{i,i'}$		14
$LT_{i,j}$	j=coal, coal-CCS, natural gas, natural gas-CCS, nuclear, hydro, onshore wind, offshore wind, solar electricity	20
	j=biomass, biomass-CCS electricity	25

	j=pumped hydro storage	6
	j=coal, coke-oven gas, natural gas, hydrogen methanol	7,8
	j=coal, coke-oven gas, natural gas, hydrogen ammonia	9,10
	j=water electrolysis	12
	j=direct air capture	13
$LT_{i,i'}$		26,27
$SL_{i,j}$	j=coal, coal-CCS, natural gas, natural gas-CCS, biomass, biomass-CCS electricity	4
	j=water electrolysis	2
$RU_{i,j}$	j=coal, coal-CCS, natural gas, natural gas-CCS, biomass, biomass-CCS electricity	4
	j=water electrolysis	2
$RD_{i,j}$	j=coal, coal-CCS, natural gas, natural gas-CCS, biomass, biomass-CCS electricity	4
	j=water electrolysis	2
$UT_{i,j}$	j=coal, coal-CCS, natural gas, natural gas-CCS, biomass, biomass-CCS electricity	27
	j=water electrolysis	2
$UP_{i,j}$	j=coal, coal-CCS, natural gas, natural gas-CCS, biomass, biomass-CCS electricity	3
	j=water electrolysis	2
$DN_{i,j}$	j=coal, coal-CCS, natural gas, natural gas-CCS, biomass, biomass-CCS electricity	3
	j=water electrolysis	2
$SSEX_{t,i,j}$	j=coal, coal-CCS, natural gas, natural gas-CCS, biomass, biomass-CCS electricity	14
	j=water electrolysis	2
$EFF_{i,j}$	j=pumped hydro storage	4
$LOSS$		28
$ELDM_{t,d,h,i}$	t=current	29,30
	t=future	31
$MEDM_{t,i}$	t=current	15
	t=future	32
$AMDM_{t,i}$	t=current	16
	t=future	33
$EXCAP_{t,i,j}$	j=coal, coal-CCS, natural gas, natural gas-CCS, nuclear, hydro, onshore wind, offshore wind, solar, biomass, biomass-CCS electricity	29
	j=pumped hydro storage	6
	j=coal, coke-oven gas, natural gas, hydrogen methanol	15
	j=coal, coke-oven gas, natural gas, hydrogen ammonia	16
$EXCAP_{t,i,i'}$		34

$POT_{t,i,j}$	j=coal, coal-CCS, natural gas, natural gas-CCS, nuclear electricity	29,31
	j=hydro electricity	29,34
	j=biomass, biomass-CCS electricity	35
	j=pumped hydro storage	6,36
	j=coal, coke-oven gas, natural gas methanol	15,32
	j=coal, coke-oven gas, natural gas ammonia	16,33
	j=direct air capture	37
	j=coal-CCS, natural gas-CCS, biomass-CCS electricity, direct air capture (carbon storage potential)	38,39
$CF_{d,i,j}$	j=hydro electricity	40
AGR_j	j=coal, coal-CCS, natural gas, natural gas-CCS, nuclear, biomass, biomass-CCS electricity	17
	j=hydro, onshore wind, offshore wind, solar electricity, pumped hydro storage	41
	j=coal, coke-oven gas, natural gas, hydrogen methanol, coal, coke-oven gas, natural gas, hydrogen ammonia	15
	j=direct air capture	37
RGR_j		37
TGT_t		42

As mentioned in Section 4 of the manuscript, the method of matrix-based LCA facilitated by the ecoinvent LCI database [27] as an intermediate is adopted in this work. Specially, if the set of processes, environmental flows and impact indicators are denoted P, E and I, respectively, the technology matrix A is defined as

$$A = (a_{j,i})_{j,i \in P} \#(46)$$

where $a_{j,i}$ is the output of process j's reference product per unit operation of process i. The intervention matrix B is defined as

$$B = (b_{k,i})_{k \in E,\, i \in P} \#(47)$$

where $b_{k,i}$ is the emission of environmental flow k per unit operation of process i. The characterization matrix C is defined as

$$C = (c_{l,k})_{l \in I,\, k \in E} \#(48)$$

where $c_{l,k}$ is the characterization factor of impact indicator l per unit emission of environmental flow k. Finally, for any given demand vector $b = (b_i)_{i \in P}$ where b_i represents the demand for reference product of process i, the corresponding impact can be assessed as

$$y = CBA^{-1}b \#(49)$$

where $y = (y_l)_{l \in I}$ and y_l is the value of impact indicator l. Leveraging on the ecoinvent database, when 100-year global warming potential (GWP-100a) is used as impact assessment method in this work, the characterization factors can be directly retrieved from the C matrix provided by the database as shown in Table 2 below.

Table 2: Impact assessment method corresponding to GWP-100a

Method	Category	Indicator	Unit
IPCC 2013	climate change	GWP 100a	kg CO2-Eq

The data sources of construction emission ($CAPEM_{i,j}$ or $CAPEM_{i,i'}$) and operation/transport emission ($POPEM_{i,j}$ and $TREM_{i,i'}$) parameters are listed in Tables 3 and 4 below, respectively. For data directly collected from database, the format of "[activity name] – [geography shortname] – [system model] – [version of the ecoinvent database]" is documented under the Source column while for data obtained from literature, relevant citations are provided. When both construction and operation emissions of the same technology are adopted from the database, to avoid double counting, the demand vector corresponding to operation phase is constructed such that $b_i = 1$ and $b_j = -a_{j,i}$ where i is the index of the particular technology and j is that of its construction phase activity. Similarly, since ecoinvent accounts for grid electricity as power source in pumped hydro storage while charging and discharging of energy storage are considered separately in the optimization model as shown in Section 1 of this document, grid electricity should also be excluded in the calculation of operation phase emission for pumped hydro storage. Finally, note that the mass balance coefficients $ELEC_{i,j}$, $METH_{i,j}$, $AMMO_{i,j}$, $HYDR_{i,j}$ and $CARB_{i,j}$, as well as negative emission parameters $NOPEM_{i,j}$ (if any), are obtained from the same sources as operation emissions.

Table 3: Data sources of construction emissions

Technology	Source
coal, coal-CCS, biomass, biomass-CCS electricity	[market for hard coal power plant]-[GLO]-[cutoff]-[v3.8]
natural gas, natural gas-CCS electricity	[market for gas power plant, combined cycle, 400MW electrical]-[GLO]-[cutoff]-[v3.8]
nuclear electricity	[nuclear power plant construction, pressure water reactor, 1000MW]-[CN]-[cutoff]-[v3.8]
hydro electricity	[market for hydropower plant, run-of-river]-[GLO]-[cutoff]-[v3.8]
onshore wind electricity	[market for wind turbine, 4.5MW, onshore]-[GLO]-[cutoff]-[v3.8] [market for wind turbine network connection, 4.5MW, onshore]-[GLO]-[cutoff]-[v3.8]
offshore wind electricity	[market for wind power plant, 2MW, offshore, fixed parts]-[GLO]-[cutoff]-[v3.8]

	[market for wind power plant, 2MW, offshore, moving parts]-[GLO]-[cutoff]-[v3.8]
solar electricity	[market for photovoltaic plant, 570kWp, multi-Si, on open ground]-[GLO]-[cutoff]-[v3.8]
pumped hydro storage	[market for hydropower plant, reservoir, non-alpine regions]-[GLO]-[cutoff]-[v3.8]
coal, coke-oven gas, natural gas, hydrogen methanol	[market for methanol factory]-[GLO]-[cutoff]-[v3.8]
coal, coke-oven gas, natural gas, hydrogen ammonia, direct air capture	[market for chemical factory, organics]-[GLO]-[cutoff]-[v3.8]
water electrolysis	[43]
transmission grid	[market for transmission network, long-distance]-[GLO]-[cutoff]-[v3.8]

Table 4: Data sources of operation and transport emissions

Technology	Source
coal electricity	[electricity production, hard coal]-[CN-PROVINCE]-[cutoff]-[v3.8] (PROVINCE denotes the shortname of any province in China in the database [44])
coal-CCS, biomass, biomass-CCS electricity	[45]
natural gas electricity	[electricity production, natural gas, combined cycle power plant]-[CN-PROVINCE]-[cutoff]-[v3.8]
natural gas-CCS electricity	[46]
nuclear electricity	[electricity production, nuclear, pressure water reactor]-[CN-PROVINCE]-[cutoff]-[v3.8]
hydro electricity	[electricity production, hydro, run-of-river]-[CN-PROVINCE]-[cutoff]-[v3.8]
onshore wind electricity	[electricity production, wind, >3MW turbine, onshore]-[CN-PROVINCE]-[cutoff]-[v3.8]
offshore wind electricity	[electricity production, wind, 1-3MW turbine, offshore]-[CN-PROVINCE]-[cutoff]-[v3.8]
solar electricity	[electricity production, photovoltaic, 570kWp open ground installation, multi-Si]-[CN-PROVINCE]-[cutoff]-[v3.8]
pumped hydro storage	[electricity production, hydro, pumped storage]-[CN-PROVINCE]-[cutoff]-[v3.8]
coal methanol	[47]
coke-oven gas methanol	[48]
natural gas methanol	[methanol production]-[GLO]-[cutoff]-[v3.8]
hydrogen methanol	[8]
coal ammonia	[ammonia production, partial oxidation, liquid]-[CN]-[cutoff]-[v3.8]

coke-oven gas ammonia	[16]
natural gas ammonia	[ammonia production, steam reforming, liquid]-[CN]-[cutoff]-[v3.8]
hydrogen ammonia	[11]
water electrolysis	[43]
direct air capture	[13]
transport	[market for transport, freight, lorry >32 metric ton, EURO4]-[RoW]-[cutoff]-[v3.8]

3. Wind and solar modeling

The hourly capacity factors of onshore and offshore wind generation can be calculated with turbine parameters from wind speed data as shown in Equations (50) – (52).

$$P_w = \begin{cases} \frac{1}{2} C_p(\lambda) \rho A v_w^3 & \text{if } v_{cut-in} \le v_w \le v_{rated} \\ P_{rated} & \text{if } v_{rated} \le v_w \le v_{cut-out} \\ 0 & \text{otherwise} \end{cases} \#(50)$$

$$v_w = v_{ref} \frac{\ln\left(\frac{H}{z_0}\right)}{\ln\left(\frac{H_{ref}}{z_0}\right)} \#(51)$$

$$CF_w = \frac{\eta_{ar} P_w}{P_{rated}} \#(52)$$

where P_w and P_{rated} are the actual and rated output power of wind turbine, respectively. C_p is the power coefficient which is a function of the tip speed ratio λ, ρ is the air density, A is the area swept by rotor blades and v_w is the wind speed at hub height extrapolated from near-surfurce measurement. v_{cut-in}, v_{rated} and $v_{cut-out}$ are the cut-in, rated and cut-out speed, respectively. H is the hub height of wind turbine and z_0 is the surface roughness length. H_{ref} and v_{ref} are the height of measurement and the corresponding wind speed data, respectively. η_{ar} is the wind farm array efficiency and CF_w is the resulting capacity factor of wind generation. The resulting annual average capacity factors of onshore and offshore wind power are shown in Fig. 1 (A) and (B), respectively. Note that since high resolution weather data at 0.1° latitude by 0.1° longitude [49] are not available on ocean, an alternative at slightly lower resolution (0.5° latitude by 0.625° longitude) [50] is used in offshore wind calculation. It is interesting to see that on the mainland area of China, despite Fig. 1 (B) generally agrees with Fig. 1 (A), low resolution data tend to lose track of hotspots that are constrained in small regions due to averaging, thus highlighting the need to use high resolution data when possible.

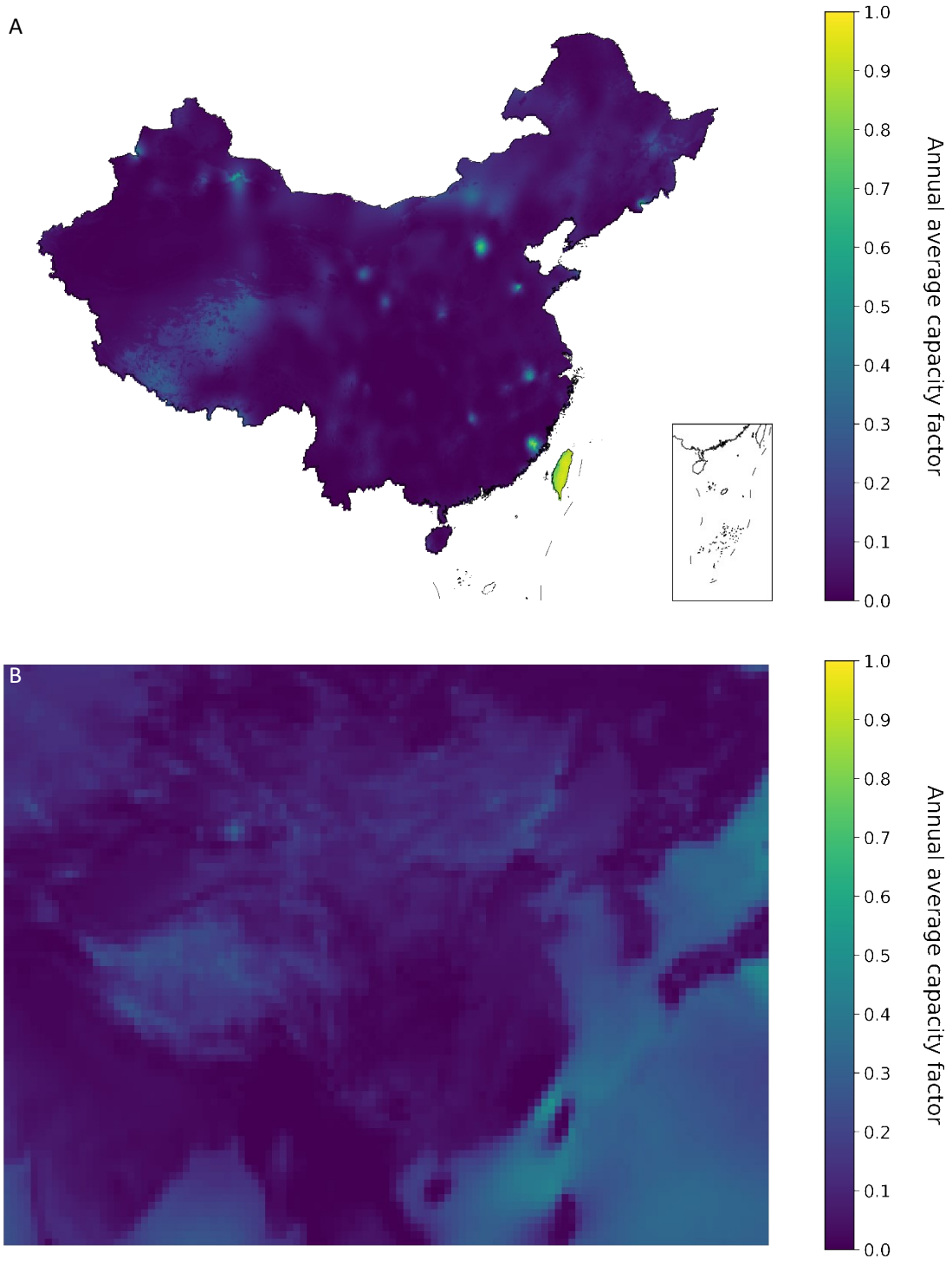

Fig. 1 Annual average capacity factors of onshore wind (A) and offshore wind (B) generation in China

For solar photovaltaic (PV) generation, ambient temperture, downward shortwave radiation and wind speed measurements are used together with device parameters for hourly capcity factor calculation as shown in Equations (53) – (64) below.

$$G_{on} = G_{sc}\left(1 + 0.033\cos\frac{360n}{365}\right) \#(53)$$

$$G_o = G_{on}\cos\theta_z \#(54)$$

where G_{sc} = 1367 W/m² is the solar constant. n represents the n[th] day of a year and G_{on} is the extraterrestrial normal radiation rate. G_o is the extraterrestrial downward radiation rate and θ_z is the zenith angle which can either be directly measured or estimated as a function of location and time as detailed in standard solar engineering textbooks [51]. With data on near-surface downward radiation (denoted G) provided [49], the sky clearness index k_T can be estimated, which further separates radiation into beam and diffuse portions.

$$k_T = \frac{G}{G_o} \#(55)$$

$$G = G_b + G_d \#(56)$$

$$\frac{G_d}{G} = \begin{cases} 1 - 0.09k_T & \text{for } k_T \le 0.22 \\ 0.9511 - 0.1604k_T + 4.388k_T^2 - 16.638k_T^3 + 12.336k_T^4 & \text{for } 0.22 < k_T \le 0.8 \\ 0.165 & \text{for } k_T > 0.8 \end{cases} \#(57)$$

$$A_i = \frac{G_b}{G_o} \#(58)$$

where G_b and G_d are the near-surface downward beam and diffuse radiation, respectively. A_i is the anisotropy index used to calculate the isotropic and circumsolar portions of diffuse radiation. Two important parameters of PV panel configuration, i.e., slope (denoted β) and azimuth angle (denoted γ), are considered in this work, from which the angle of incidence between solar radiation and PV panel (denoted θ) can be calculated using geometry [51]. The total radiation received by a tilted plane G_T is then computed as follows.

$$R_b = \frac{\cos\theta}{\cos\theta_z} \#(59)$$

$$G_T = (G_b + G_d A_i)R_b + G_d(1 - A_i)\left(\frac{1 + \cos\beta}{2}\right)\left[1 + \sqrt{\frac{G_b}{G}}\sin^3\left(\frac{\beta}{2}\right)\right] + G\rho_g\left(\frac{1 - \cos\beta}{2}\right) \#(60)$$

where R_b is the beam ratio and ρ_g is the surface reflectivity. Finally, the performance of a PV panel is not only a function of total incident radiation, but also (negatively) affected by cell temperature as shown by Equations (61) – (64).

$$T_m = G_T\exp\left(a + bv_{w10}\right) + T_a \#(61)$$

$$T_c = T_m + \left(\frac{G_T}{G_{STC}}\right)\Delta T_{cnd} \#(62)$$

$$P = P_{STC}\left(\frac{G_T}{G_{STC}}\right)\left[1 - \delta(T_{STC} - T_c)\right] \times PR \#(63)$$

$$CF_s = \frac{P}{P_{STC}} \#(64)$$

where T_m and T_c are the module back and cell temperature, respectively. a, b and ΔT_{cnd} are empirically fitted parameters with their values for different types of PV panels available in [52]. v_{w10} and T_a are the wind speed at 10-meter height and ambient temperature, respectively. G_{STC} = 1000 W/m^2, T_{STC} = 25°C and P_{STC} are the reference radiation, cell temperature and rated output power of PV panel at standard test conditions, respectively. P is the actual output power, δ is the power temperature coefficient and PR is the performance ratio. CF_s is the resulting capacity factor of solar generation. Under the assumption of fixed installation in this work, PV panels are mounted South as China is located in the Northern Hemisphere. The optimal slope in terms of highest annual average capacity factor is computed for each 0.1° latitude by 0.1° longitude grid cell with available weather data [49] as shown in Fig. 2 (A) and (B) below.

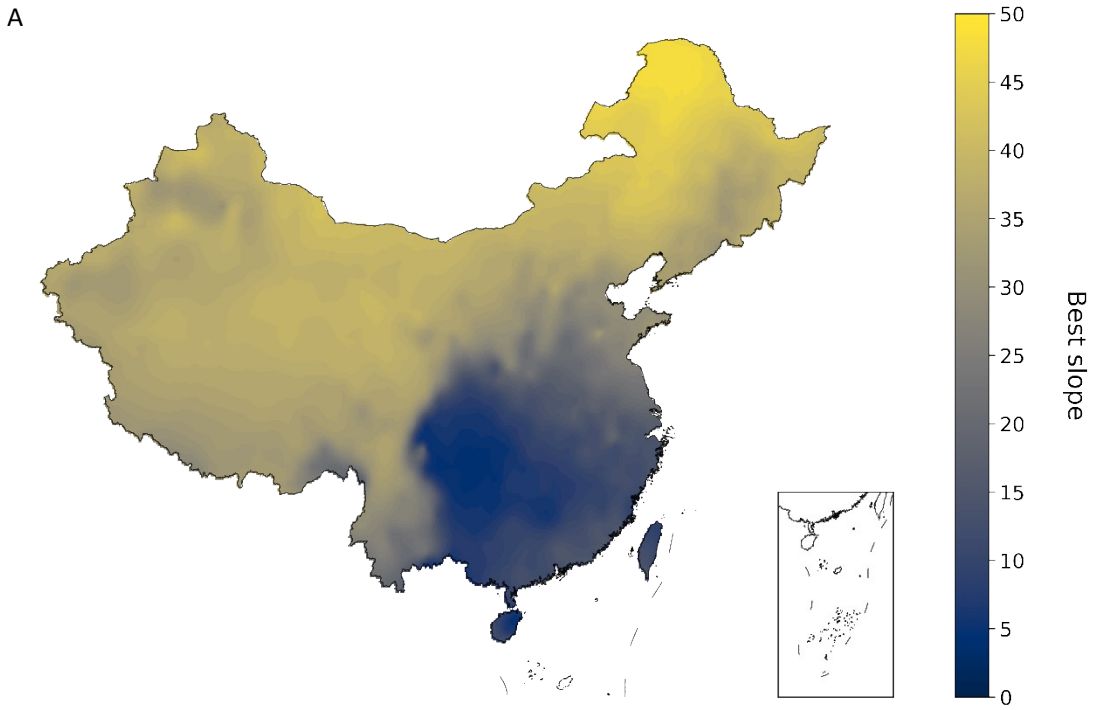

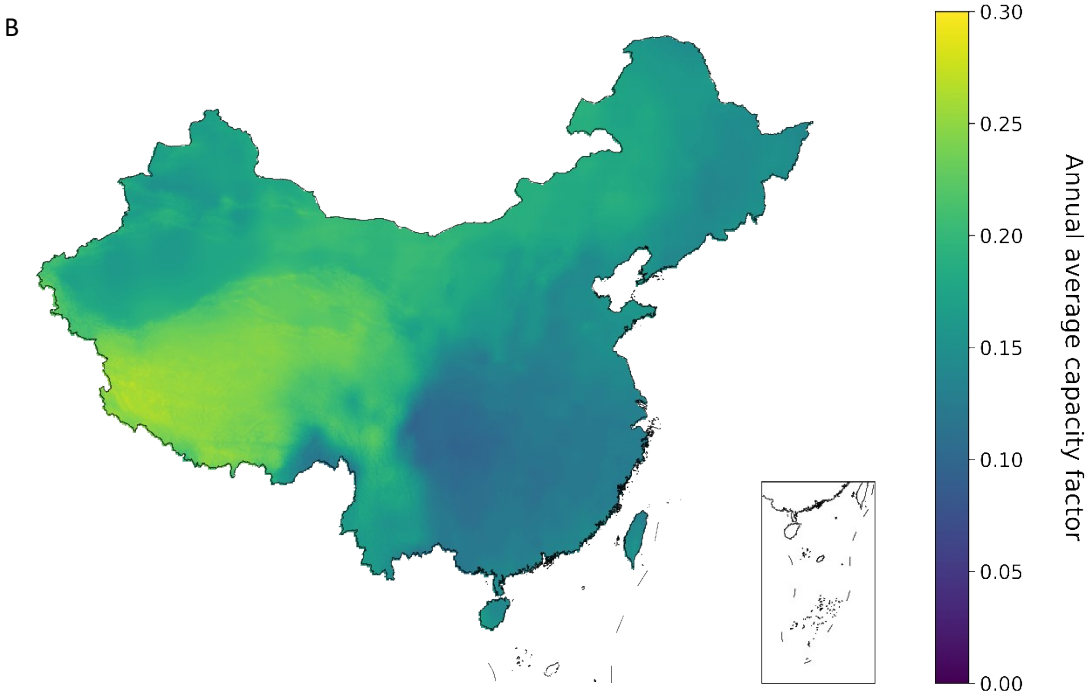

Fig. 2 Best installation slopes of PV panel (A) and the corresponding annual average capacity factors (B) in China

Regarding the installation potential of onshore wind and solar generation in China, gridded terrain (slope and elevation) [53] and land cover [54] data are used together with weather data [49] to pick out the suitable area for each type of renewable development. For every grid cell i with available data, the general formula to compute the maximum installation capacity CP_i is given by Equation (65).

$$CP_i = a_i \times f_i \times \eta_i \#(65)$$

where a_i is the area of grid cell i, f_i is the overall suitability factor considering terrain, land cover and weather conditions and η_i is the installation intensity.

Depending on the aggressiveness of estimation, various values of f_i and η_i have been witnessed in literature [55]. In this work, moderate assumptions on suitability factors and installation intensities are generally adopted as documented in the following. Firstly, protected land areas [56] are excluded from the calculation of renewable development potential. For terrain filters, slope and elevation data are obtained from [53] with the requirements of slope < 5% and elevation < 3000 m enforced on the estimation of both onshore wind [57] and solar [58] potentials. For land cover filters that are shown in Table 5 below, land cover data are adopted from [54] with (onshore) wind suitability factors and roughness length values collected from [59] and solar suitability factors obtained from [58]. For weather filters, annual average wind speed at hub height (100 m) > 6 m/s [57] and annual average solar radiation > 160 W/m^2 [60] are used for wind and solar development, respectively. Lastly, a turbine installation intensity of 4 MW/km^2 is applied to onshore wind potential estimation. Regarding maximum solar capacity, a PV efficiency of 0.17 is assumed. For locations with high PV installation slope, the heuristic of no shading at solar noon on the winter solstice [61] is used to

calculate the corresponding packing factors of solar PV while for locations with low installation slope, a constant value of 0.47 is assumed [62].

Table 5: Land cover filters for onshore wind and solar potential estimation

Land cover	Wind suitability factor	Roughness length (m)	Solar suitability factor
water	0	0.005	0
evergreen needleleaf forest	0.1	1	0
evergreen broadleaf forest	0	1	0
deciduous needleleaf forest	0.1	1	0
deciduous broadleaf forest	0.1	1	0
mixed forests	0.1	1	0
closed shrubland	0.5	0.1	0.03
open shrublands	0.5	0.1	0.15
woody savannas	0.9	0.25	0.03
savannas	0.9	0.25	0.15
grasslands	0.8	0.515	0.15
permanent wetlands	0	0.005	0
croplands	0.7	0.25	0
urban and built-up	0	0.005	0.03
cropland/natural vegetation mosaic	0.7	0.25	0
snow and ice	0	0.005	0
barren or sparsely vegetated	1	0.005	0.15

Regarding offshore wind installation potential, the same Equation (65) can be applied but the overall suitability factor f_i consists of different components. Firstly, only the grid cells that are offshore [63] and fall within China's Exclusive Economic Zone (EEZ) [64] can be considered. With bathymetry data obtained from [65], a filter of bathymetry > -20 m [57] is applied. Besides, the same weather filter of annual average wind speed at hub height > 6 m/s and installation intensity of 4 MW/km^2 as those for onshore wind are adopted in estimating offshore wind potential as well. Finally, the overall results of wind (onshore + offshore) and solar development potential estimation in China are visualized in Fig. 3 (A) and (B), respectively.

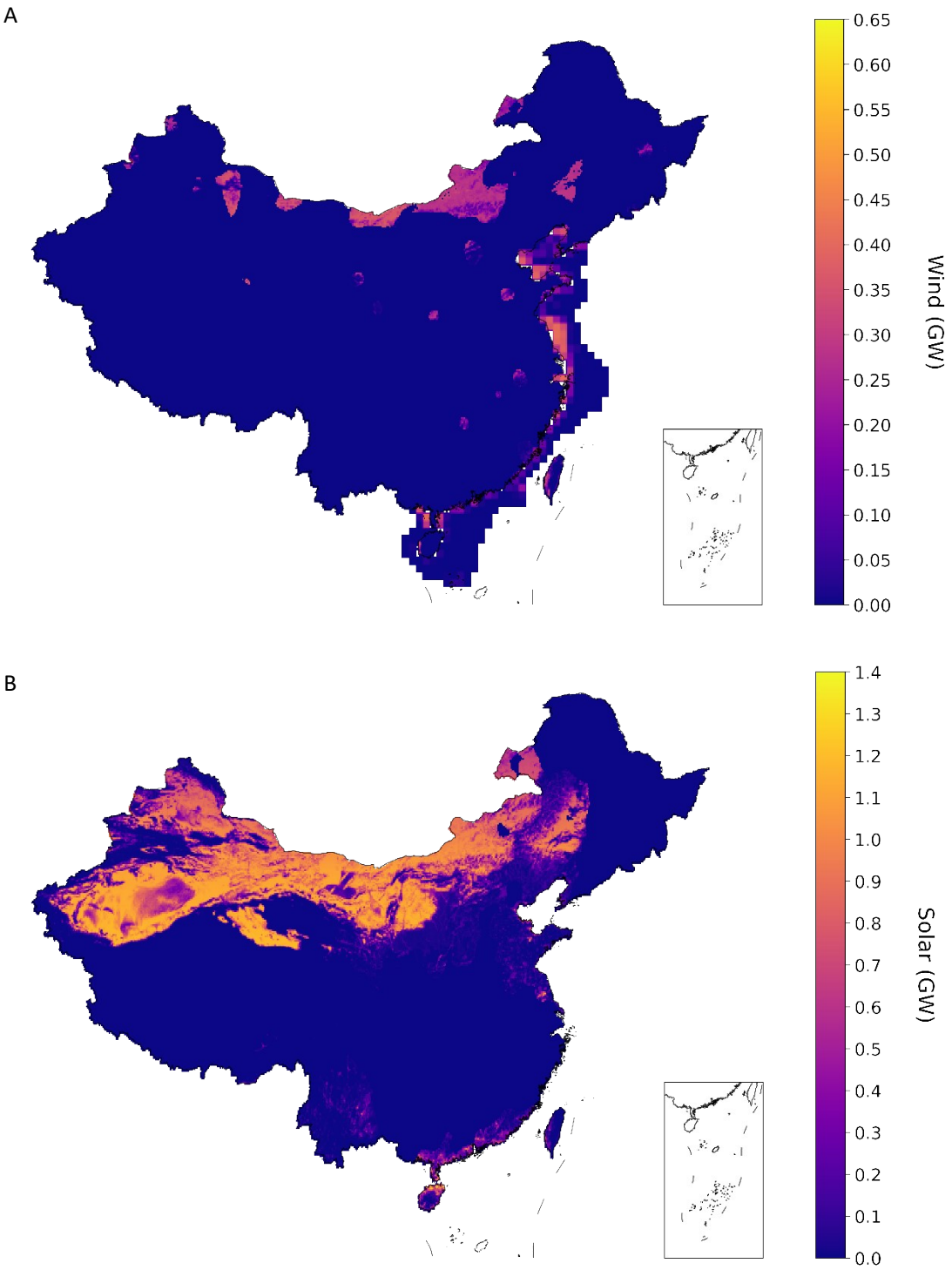

Fig. 3 Installation potential of onshore and offshore wind (A) and solar (B) generation in China

Given the relatively high spatial resolution of renewable potential results above, it is common that a province in China covers multiple grid cells. The provincial capacity factors $ECF_{t,d,h,i,j}$ and $FCF_{t,d,h,i,j}$ can thus be obtained by averaging over locations that are already developed and available for future developments, respectively, weighted by existing or potential installation capacities. The distributions of annual average capacity factors of all (suitable) grid cells within each province are plotted in Fig. 4 – 6 for onshore wind, offshore wind and solar generation,

respectively.

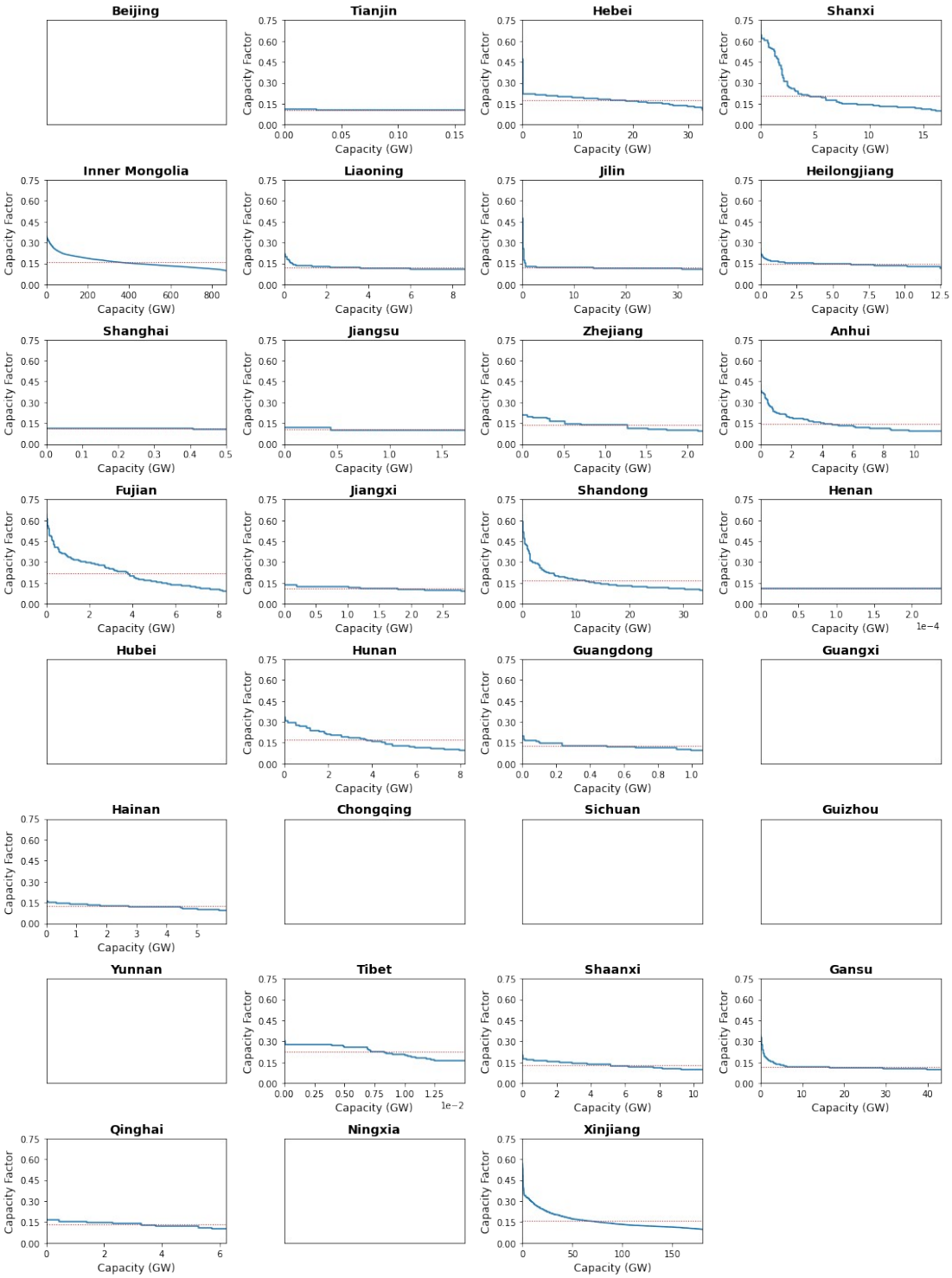

Fig. 4 Distribution of annual average onshore wind capacity factors of all grid cells in each province. Red dotted lines denote provincial average values.

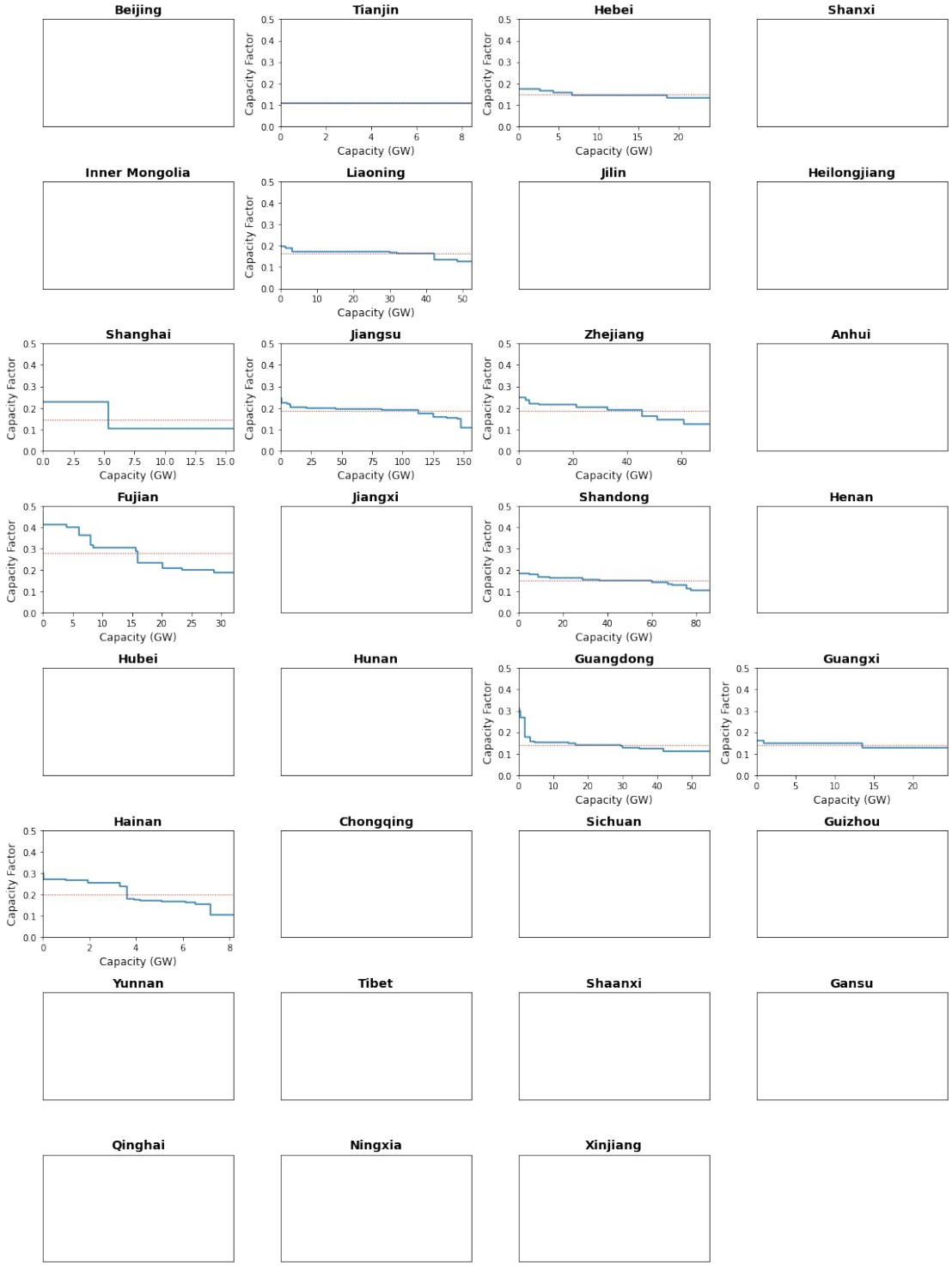

Fig. 5 Distribution of annual average offshore wind capacity factors of all grid cells in each province. Red dotted lines denote provincial average values.

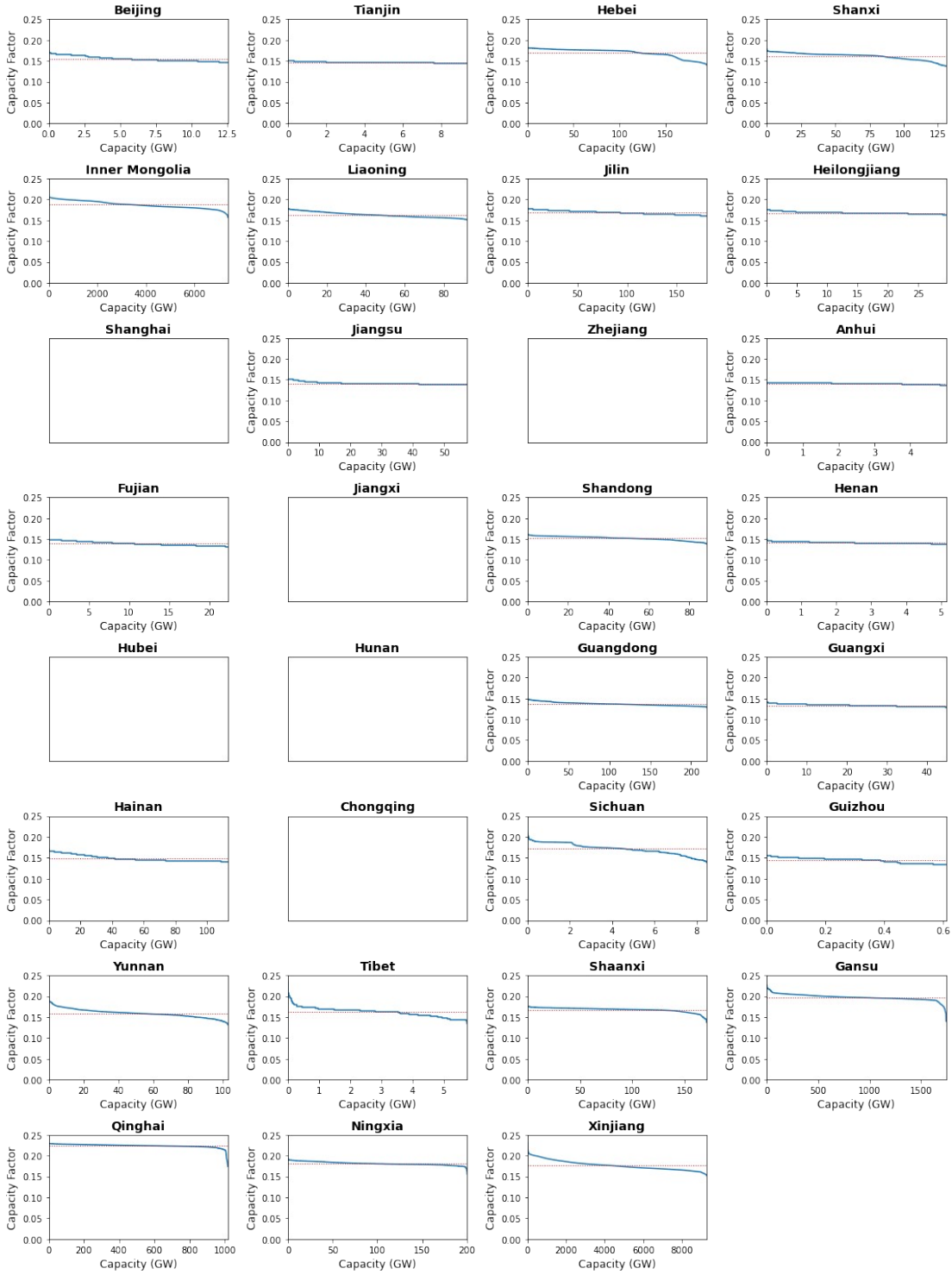

Fig. 6 Distribution of annual average solar capacity factors of all grid cells in each province. Red dotted lines denote provincial average values.

Finally, the per-month typical-day hourly capacity factors of onshore wind, offshore wind and solar generation for each province are plotted in Fig. 7 – 9, respectively. The profile curves are obtained by averaging over all grid cells in a province, weighted by their corresponding maximum installation (i.e., potential) capacities.

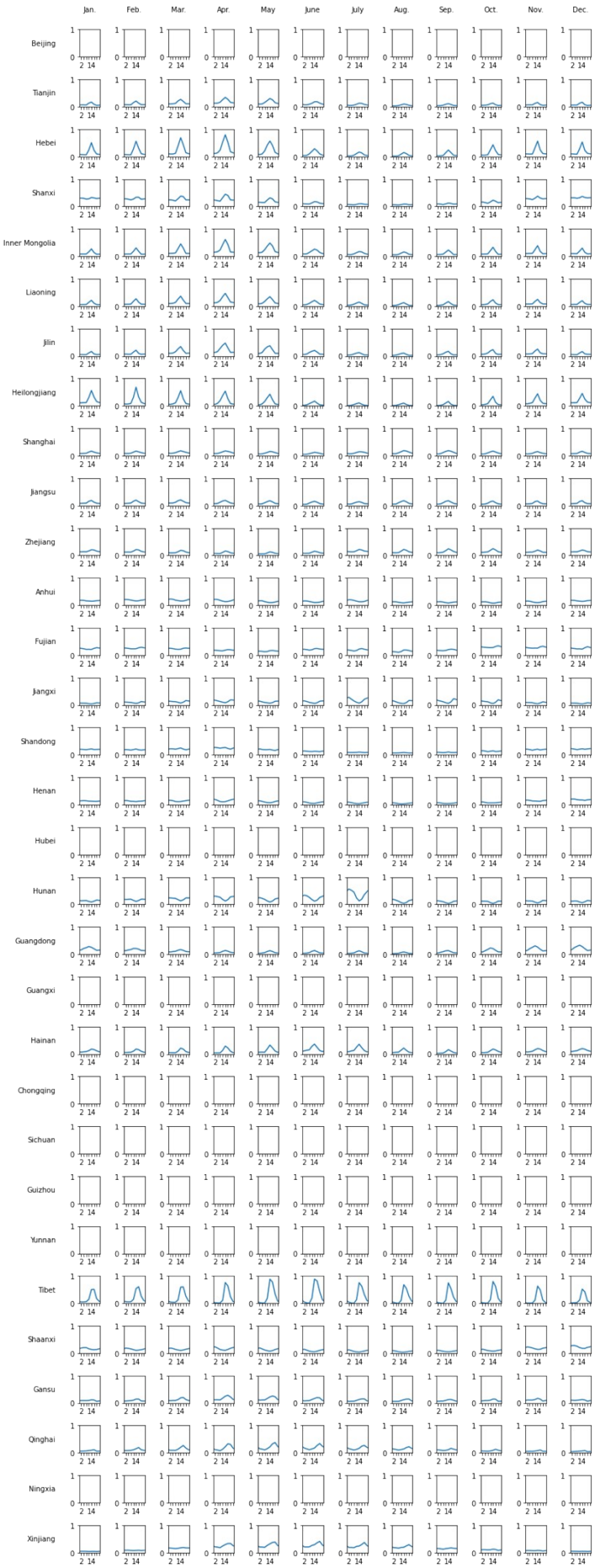
Jan.
Feb.
Mar.
Apr.
May
June
July
Aug.
Sep.
Oct.
Nov.
Dec.
Beijing
Tianjin
Hebei
Shanxi
Inner Mongolia
Liaoning
Jilin
Heilongjiang
Shanghai
Jiangsu
Zhejiang
Anhui
Fujian
Jiangxi
Shandong
Henan
Hubei
Hunan
Guangdong
Guangxi
Hainan
Chongqing
Sichuan
Guizhou
Yunnan
Tibet
Shaanxi
Gansu
Qinghai
Ningxia
Xinjiang
1
0
2
14

Fig. 7 Typical day onshore wind capacity factors averaged over all grid cells in each province. Horizonal and vertical axes denote hour and capacity factor, respectively.

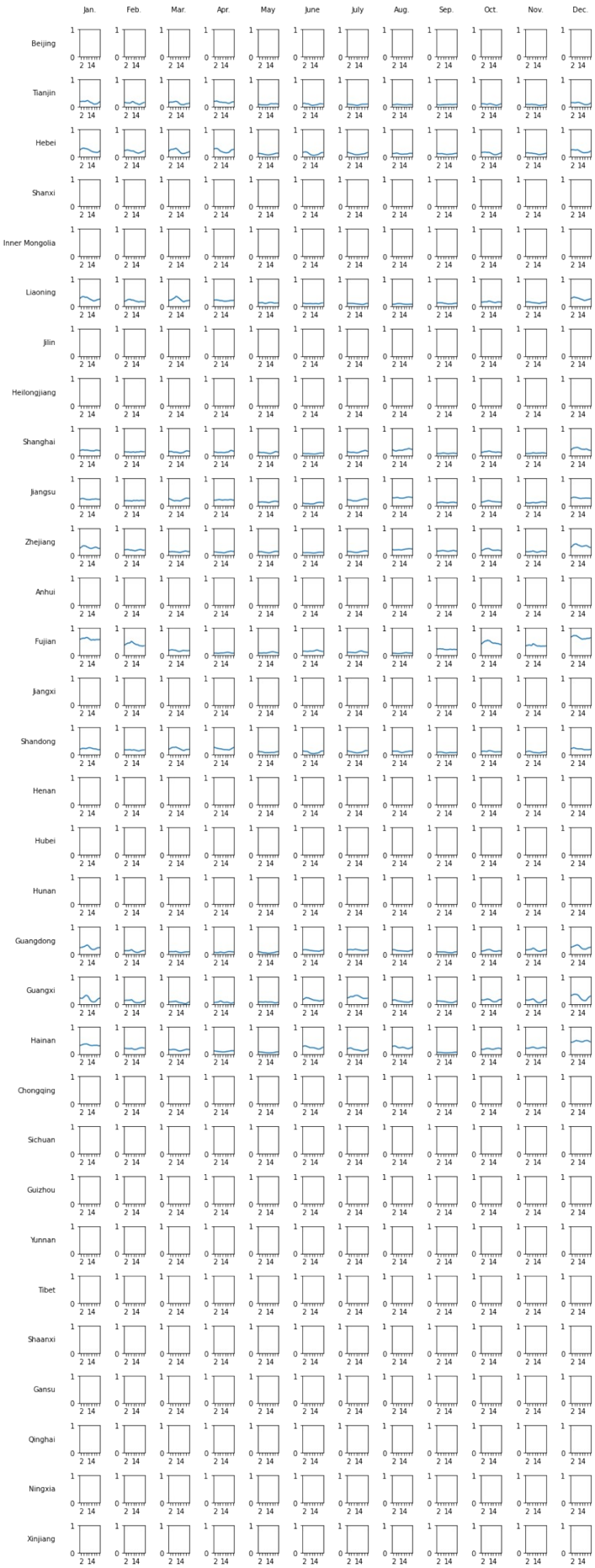
Jan.
Feb.
Mar.
Apr.
May
June
July
Aug.
Sep.
Oct.
Nov.
Dec.
Beijing
Tianjin
Hebei
Shanxi
Inner Mongolia
Liaoning
Jilin
Heilongjiang
Shanghai
Jiangsu
Zhejiang
Anhui
Fujian
Jiangxi
Shandong
Henan
Hubei
Hunan
Guangdong
Guangxi
Hainan
Chongqing
Sichuan
Guizhou
Yunnan
Tibet
Shaanxi
Gansu
Qinghai
Ningxia
Xinjiang
1
0
2
14

Fig. 8 Typical day offshore wind capacity factors averaged over all grid cells in each province. Horizonal and vertical axes denote hour and capacity factor, respectively.

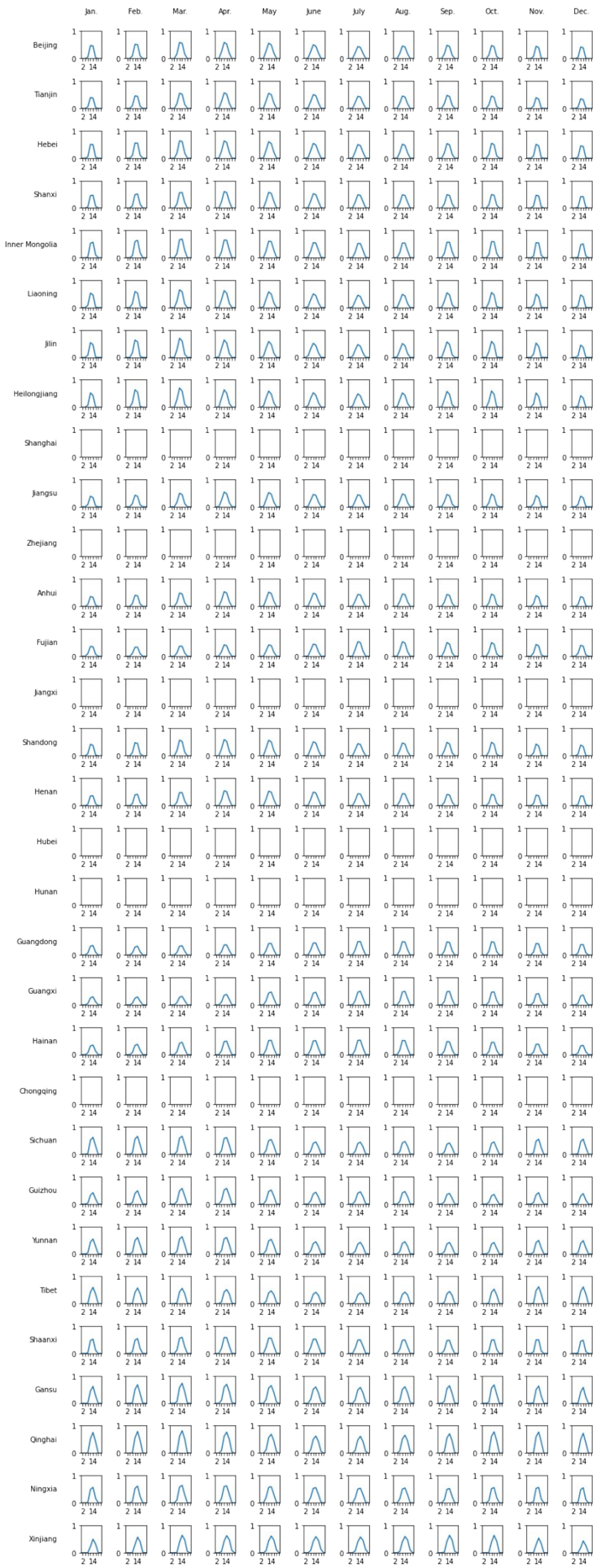
Jan.
Feb.
Mar.
Apr.
May
June
July
Aug.
Sep.
Oct.
Nov.
Dec.
Beijing
Tianjin
Hebei
Shanxi
Inner Mongolia
Liaoning
Jilin
Heilongjiang
Shanghai
Jiangsu
Zhejiang
Anhui
Fujian
Jiangxi
Shandong
Henan
Hubei
Hunan
Guangdong
Guangxi
Hainan
Chongqing
Sichuan
Guizhou
Yunnan
Tibet
Shaanxi
Gansu
Qinghai
Ningxia
Xinjiang
1
0
2
14

Fig. 9 Typical day solar capacity factors averaged over all grid cells in each province. Horizonal and vertical axes denote hour and capacity factor, respectively.

Reference

1 J. D. Jenkins and N. A. Sepulveda, *Enhanced Decision Support for a Changing Electricity Landscape: The GenX Configurable Electricity Resource Capacity Expansion Model*, 2017.

2 G. He, D. S. Mallapragada, A. Bose, C. F. Heuberger and E. Gencer, *IEEE Trans. Sustain. Energy*, 2021, **12**, 1730–1740.

3 W. Zappa, M. Junginger and M. van den Broek, *Appl. Energy*, 2019, **233**–**234**, 1027–1050.

4 R. Jing, X. Wang, Y. Zhao, Y. Zhou, J. Wu and J. Lin, *Adv. Appl. Energy*, 2021, **3**, 100053.

5 IEA, *World Energy Outlook 2020*, Paris, 2020.

6 Energy Foundation, *Study on Pumped Hydro Storage to Promote the Consumption of Wind and Solar Power in China*, 2021.

7 M. Woods, N. Kuehn, V. Shah, C. W. White lll and J. F. Goellner, *Baseline Analysis of Crude Methanol Production from Coal and Natural Gas*, 2014.

8 M. Pérez-Fortes, J. C. Schöneberger, A. Boulamanti and E. Tzimas, *Appl. Energy*, 2016, **161**, 718–732.

9 D. C. C. Habgood, A. F. A. Hoadley and L. Zhang, *Chem. Eng. Res. Des.*, 2015, **102**, 57–68.

10 R. J. Lee Pereira, P. A. Argyris and V. Spallina, *Appl. Energy*, 2020, **280**, 115874.

11 E. R. Morgan, *Open Access Diss.*, 2013, 697.

12 IEA, *The Future of Hydrogen*, Paris, 2019.

13 D. W. Keith, G. Holmes, D. St. Angelo and K. Heidel, *Joule*, 2018, **2**, 1573–1594.

14 Y. Yang, H. Zhang, W. Xiong, D. Zhang and X. Zhang, *Environ. Impact Assess. Rev.*, 2018, **73**, 142–151.

15 Y. Li, S. Lan, J. Pérez-Ramírez and X. Wang, *Sustain. Energy Fuels*, 2020, **4**, 6141–6155.

16 Y. Li, S. Lan, M. Ryberg, J. Pérez-Ramírez and X. Wang, *iScience*, 2021, **24**, 102513.

17 R. Cheng, Z. Xu, P. Liu, Z. Wang, Z. Li and I. Jones, *Appl. Energy*, 2015, **137**, 413–426.

18 C. F. Heuberger, E. S. Rubin, I. Staffell, N. Shah and N. Mac Dowell, *Appl. Energy*, 2017, **204**, 831–845.

19 M. B. Lieberman, *RAND J. Econ.*, 1984, **15**, 213.

20 IEA, *Projected Costs of Generating Electricity 2020*, Paris, 2020.

21 Price of biomass fuels in China, https://www.sohu.com/a/271751001_422316, (accessed 26 February 2021).

22 A. Bhave, R. H. S. Taylor, P. Fennell, W. R. Livingston, N. Shah, N. Mac Dowell, J. Dennis, M. Kraft, M. Pourkashanian, M. Insa, J. Jones, N. Burdett, A. Bauen, C. Beal, A. Smallbone and J. Akroyd, *Appl. Energy*, 2017, **190**, 481–489.

23 U.S. Energy Information Administration, Annual Energy Outlook 2021, https://www.eia.gov/outlooks/aeo/data/browser/, (accessed 26 February 2021).

24 National Bureau of Statistics, National Data - Price Index for Transport and Communications, https://data.stats.gov.cn/easyquery.htm?cn=A01&zb=A010201&sj=202103, (accessed 21 April 2021).

25 IRENA, *Renewable Power Generation Costs in 2018*, International Renewable Energy Agency, Abu Dhabi, 2019.

26 R. Itten, R. Frischknecht and M. Stucki, *Life Cycle Inventories of Electricity Mixes and Grid*, 2012.

27 G. Wernet, C. Bauer, B. Steubing, J. Reinhard, E. Moreno-Ruiz and B. Weidema, *Int. J. Life Cycle Assess.*, 2016, **21**, 1218–1230.

28 A. Galán-Martín, C. Pozo, A. Azapagic, I. E. Grossmann, N. Mac Dowell and G. Guillén-Gosálbez,

Energy Environ. Sci., 2018, **11**, 572–581.
29 CEPY, *China Electric Power Yearbook*, China Electric Power Press, Beijing, 2018.
30 National Development and Reform Commission, Typical power load curves of provincial power grids, http://www.gov.cn/xinwen/2019-12/30/content_5465088.htm, (accessed 7 September 2022).
31 State Grid Energy Research Institute, China Energy and Electricity Outlook, https://news.bjx.com.cn/html/20201202/1119479.shtml, (accessed 30 April 2021).
32 Argus, *Argus Global Methanol Annual 2018*, 2018.
33 H. Yang, *China Chem. Report.*, 2020, **31**, 10–12.
34 China Electric Power Enterprise Federation, *Annual Development Report on China's Electric Power Industry*, 2021.
35 Y. Kang, Q. Yang, P. Bartocci, H. Wei, S. S. Liu, Z. Wu, H. Zhou, H. Yang, F. Fantozzi and H. Chen, *Renew. Sustain. Energy Rev.*, 2020, **127**, 109842.
36 National Energy Administration, Medium and Long-term Development Plan of Pumped Hydro Storage, http://www.gov.cn/xinwen/2021-09/09/content_5636487.htm, (accessed 4 September 2022).
37 G. Realmonte, L. Drouet, A. Gambhir, J. Glynn, A. Hawkes, A. C. Köberle and M. Tavoni, *Nat. Commun.*, 2019, **10**, 1–12.
38 X. Li, N. Wei, Y. Liu, Z. Fang, R. T. Dahowski and C. L. Davidson, *Energy Procedia*, 2009, **1**, 2793–2800.
39 N. Wei, X. Li, Z. Fang, B. Bai, Q. Li, S. Liu and Y. Jia, *J. CO2 Util.*, 2015, **11**, 20–30.
40 State Power, Monthly Electricity Production of Hydropower in China, https://www.ceicdata.com/.
41 Energy Foundation, China 2050 High Renewable Energy Penetration Scenario and Roadmap Study, https://www.efchina.org/Reports-zh/china-2050-high-renewable-energy-penetration-scenario-and-roadmap-study-zh, (accessed 26 February 2021).
42 X. Zhang, in *12th International Conference on Applied Energy*, 2020.
43 Icelandic New Energy, *Generation of the energy carrier hydrogen – in context with electricity buffering generation through fuel cells*, 2008.
44 ecoinvent, List of Geographies Present in ecoinvent 3, https://www.ecoinvent.org/support/documents-and-files/documents-and-files.html, (accessed 26 August 2020).
45 B. Yang, Y. M. Wei, Y. Hou, H. Li and P. Wang, *Appl. Energy*, 2019, **252**, 113483.
46 B. Singh, A. H. Strømman and E. Hertwich, *Int. J. Greenh. Gas Control*, 2011, **5**, 457–466.
47 Z. Qin, G. Zhai, X. Wu, Y. Yu and Z. Zhang, *Energy Convers. Manag.*, 2016, **124**, 168–179.
48 C. Li, H. Bai, Y. Lu, J. Bian, Y. Dong and H. Xu, *J. Clean. Prod.*, 2018, **188**, 1004–1017.
49 J. He, K. Yang, W. Tang, H. Lu, J. Qin, Y. Chen and X. Li, *Sci. Data 2020 71*, 2020, **7**, 1–11.
50 Global Modeling and Assimilation Office (GMAO), 2015.
51 J. A. Duffie, W. A. Beckman and N. Blair, 931.
52 T. Dierauf, A. Growitz, S. Kurtz, J. L. B. Cruz, E. Riley and C. Hansen, , DOI:10.2172/1078057.
53 G. Fischer, F. Nachtergaele, S. Prieler, H. T. van Velthuizen, L. Verelst and D. Wiberg, Global Agro-ecological Zones Assessment for Agriculture (GAEZ 2008), https://www.fao.org/soils-portal/data-hub/soil-maps-and-databases/harmonized-world-soil-database-v12/en/, (accessed 15 October 2021).

54 M. A. Friedl and D. Sulla-Menashe, MCD12C1 MODIS/Terra+Aqua Land Cover Type Yearly L3 Global 0.05Deg CMG V006, https://doi.org/10.5067/MODIS/MCD12C1.006, (accessed 14 September 2021).
55 P. A. Adedeji, S. A. Akinlabi, N. Madushele and O. O. Olatunji, *J. Clean. Prod.*, 2020, **269**, 122104.
56 Protected Planet, Explore the World's Protected Areas, https://www.protectedplanet.net/en, (accessed 15 October 2021).
57 G. He and D. M. Kammen, *Energy Policy*, 2014, **74**, 116–122.
58 S. Chen, X. Lu, Y. Miao, Y. Deng, C. P. Nielsen, N. Elbot, Y. Wang, K. G. Logan, M. B. McElroy and J. Hao, *Joule*, 2019, **3**, 1895–1912.
59 M. M. Hoogwijk, .
60 G. He and D. M. Kammen, *Renew. Energy*, 2016, **85**, 74–82.
61 W. Zappa and M. van den Broek, *Renew. Sustain. Energy Rev.*, 2018, **94**, 1192–1216.
62 D. E. H. J. Gernaat, H. S. de Boer, V. Daioglou, S. G. Yalew, C. Müller and D. P. van Vuuren, *Nat. Clim. Chang. 2021 112*, 2021, **11**, 119–125.
63 Food and Agriculture Organization of the United Nations, Harmonized world soil database v1.2, https://www.fao.org/soils-portal/data-hub/soil-maps-and-databases/harmonized-world-soil-database-v12/en/, (accessed 27 April 2022).
64 Flanders Marine Institute, Marine Regions - Chinese Exclusive Economic Zone (EEZ), https://www.marineregions.org/gazetteer.php?p=details&id=8486, (accessed 5 September 2022).
65 International Hydrographic Organization and Intergovernmental Oceanographic Commission, GEBCO Gridded Bathymetry Data, https://www.gebco.net/data_and_products/gridded_bathymetry_data/, (accessed 5 September 2022).